# Ancestral Reconstruction of Karyotypes Reveals an Exceptional Rate of Nonrandom Chromosomal Evolution in Sunflower

**Kate L. Ostevik,*,†,1 Kieran Samuk,* and Loren H. Rieseberg†**

*Department of Biology, Duke University, Durham, North Carolina 27701 and †Department of Botany, University of British Columbia, Vancouver, British Columbia V6T 1Z4, Canada

ORCID IDs: 0000-0002-2197-9284 (K.L.O.); 0000-0003-0396-465X (K.S.); 0000-0002-2712-2417 (L.H.R.)

**ABSTRACT** Mapping the chromosomal rearrangements between species can inform our understanding of genome evolution, reproductive isolation, and speciation. Here, we present a novel algorithm for identifying regions of synteny in pairs of genetic maps, which is implemented in the accompanying R package syntR. The syntR algorithm performs as well as previous *ad hoc* methods while being systematic, repeatable, and applicable to mapping chromosomal rearrangements in any group of species. In addition, we present a systematic survey of chromosomal rearrangements in the annual sunflowers, which is a group known for extreme karyotypic diversity. We build high-density genetic maps for two subspecies of the prairie sunflower, *Helianthus petiolaris* ssp. *petiolaris* and *H. petiolaris* ssp. *fallax*. Using syntR, we identify blocks of synteny between these two subspecies and previously published high-density genetic maps. We reconstruct ancestral karyotypes for annual sunflowers using those synteny blocks and conservatively estimate that there have been 7.9 chromosomal rearrangements per million years, a high rate of chromosomal evolution. Although the rate of inversion is even higher than the rate of translocation in this group, we further find that every extant karyotype is distinguished by between one and three translocations involving only 8 of the 17 chromosomes. This nonrandom exchange suggests that specific chromosomes are prone to translocation and may thus contribute disproportionately to widespread hybrid sterility in sunflowers. These data deepen our understanding of chromosome evolution and confirm that *Helianthus* has an exceptional rate of chromosomal rearrangement that may facilitate similarly rapid diversification.

**KEYWORDS** chromosomal rearrangement; synteny block; *Helianthus*; syntR; dot plot

ORGANISMS vary widely in the number and arrangement of their chromosomes, *i.e.*, their karyotype. Interestingly, karyotypic differences are often associated with species boundaries and, therefore, suggest a link between chromosomal evolution and speciation (White 1978; King 1993). Indeed, it is well established that chromosomal rearrangements can contribute to reproductive isolation. Individuals heterozygous for divergent karyotypes are often sterile or inviable (King 1987; Lai *et al.* 2005; Stathos and Fishman 2014). Apart from directly causing hybrid sterility and inviability, chromosomal rearrangements can also facilitate the evolution of other reproductive barriers by extending genomic regions that are protected from introgression (Noor *et al.* 2001; Rieseberg 2001), accumulating genetic incompatibilities (Navarro and Barton 2003), and simplifying reinforcement (Trickett and Butlin 1994). Despite its prevalence and potentially important role in speciation, the general patterns of karyotypic divergence are still not well understood. Mapping and characterizing chromosomal rearrangements in many taxa is a critical step toward understanding their evolutionary dynamics.

The genus *Helianthus* (sunflowers) is well known to have particularly labile genome structure, and is thus a viable system in which to map and characterize a variety of rearrangements. These sunflowers have several paleopolyploidy events in their evolutionary history (Barker *et al.* 2008, 2016; Badouin *et al.* 2017), have given rise to three homoploid hybrid species (Rieseberg 1991), and are prone to transposable element activity (Kawakami *et al.* 2011; Staton *et al.*


doi: https://doi.org/10.1534/genetics.120.303026
Manuscript received August 15, 2019; accepted for publication February 3, 2020; published Early Online February 7, 2020.
Supplemental material available at figshare: https://doi.org/10.25386/genetics.11819625.
[1]Corresponding author: Box 90338, 137 Biological Sciences, Duke University, 130 Science Dr., Durham, NC 27708. E-mail: kate.ostevik@gmail.com

2012). Evidence in the form of hybrid pollen inviability, abnormal chromosome pairings during meiosis, and genetic map comparisons suggests that *Helianthus* karyotypes are unusually diverse (Heiser 1947, 1951, 1961; Whelan 1979; Chandler *et al.* 1986; Quillet *et al.* 1995; Rieseberg *et al.* 1995; Burke *et al.* 2004; Heesacker *et al.* 2009; Barb *et al.* 2014). In fact, annual sunflowers have one of the highest described rates of chromosomal evolution across all plants and animals (Burke *et al.* 2004).

Studying chromosomal evolution within any group requires high-density genetic maps. Recently, Barb *et al.* (2014) built high-density genetic maps for the sunflower species *Helianthus niveus* ssp. *tephrodes* and *H. argophyllus*, and compared them to *H. annuus*. This analysis precisely mapped previously inferred karyotypes (Heiser 1951; Chandler *et al.* 1986; Quillet *et al.* 1995), but only captured a small amount of the chromosomal variation in the annual sunflowers. For example, comparisons of genetic maps with limited marker density suggest that several chromosomal rearrangements differentiate *H. petiolaris* from *H. annuus* (Rieseberg *et al.* 1995; Burke *et al.* 2004), and evidence from cytological surveys suggests that subspecies within *H. petiolaris* subspecies carry divergent karyotypes (Heiser 1961). Adding high-density genetic maps of *H. petiolaris* subspecies to the Barb *et al.* (2014) analysis will allow us to: (1) precisely track additional rearrangements, (2) reconstruct ancestral karyotypes for the group, and (3) untangle overlapping rearrangements that can be obscured by directly comparing present-day karyotypes.

Another critical part of a multispecies comparative study of chromosome evolution using genetic map data is a systematic and repeatable method for identifying syntenic chromosomal regions (*sensu* Pevzner and Tesler 2003). These methods are especially important for cases with high marker density because breakpoints between synteny blocks can be blurred by mapping errors, microrearrangements, and paralogy (Hackett and Broadfoot 2003; Choi *et al.* 2007; Barb *et al.* 2014; Bilton *et al.* 2018). In previous studies, synteny blocks have been found by a variety of *ad hoc* methods, including counting all differences in marker order (Wu and Tanksley 2010), by visual inspection (Burke *et al.* 2004; Marone *et al.* 2012; Latta *et al.* 2019), or by manually applying simple rules like size thresholds (Heesacker *et al.* 2009; Barb *et al.* 2014; Rueppell *et al.* 2016) and Spearman's rank comparisons (Berdan *et al.* 2014; Schlautman *et al.* 2017). However, these methods become intractable and prone to error when applied to very-dense genetic maps. Furthermore, to our knowledge, there is no software available that identifies synteny blocks based on relative marker positions alone (*i.e.*, without requiring reference genomes, sequence data, or markers with known orientations).

Here, with the goal of understanding chromosome evolution in *Helianthus* and more generally, we aimed to: (1) build high-density genetic maps for two subspecies of *H. petiolaris*, (2) develop a method and software to systematically and repeatably identify synteny blocks from any number of paired genetic map positions, (3) reconstruct ancestral karyotypes for a subsection of annual sunflowers, and (4) detect general patterns of chromosomal rearrangement in *Helianthus*.

## Materials and Methods

### *Study system*

We focused on five closely related diploid ($2n = 34$) taxa from the annual clade of the genus *Helianthus* (Figure 1). These sunflowers are native to North America (Supplemental Material, Figure S1; Rogers *et al.* 1982) and are naturally self-incompatible (domesticated lineages of *H. annuus* are self-compatible). *H. annuus* occurs throughout much of the central US states, often in somewhat heavy soils and along roadsides (Heiser 1947). *H. petiolaris* occurs in sandier soils and is made up of two subspecies: *H. petiolaris* ssp. *petiolaris*, which is commonly found in the southern Great Plains, and *H. petiolaris* ssp. *fallax*, which is limited to more arid regions in Colorado, Utah, New Mexico, and Arizona (Heiser 1961). Where *H. petiolaris* and *H. annuus* are sympatric, gene flow occurs between the species (Strasburg and Rieseberg 2008). *H. argophyllus* is primarily found along the east coast of Texas, where it also overlaps and hybridizes with *H. annuus* (Baute *et al.* 2016). Finally, *H. niveus* ssp. *tephrodes* is a facultative perennial that grows in dunes from the southwestern US states into Mexico.

### *Controlled crosses*

To make genetic maps, we crossed an outbred individual with presumably high heterozygosity from each *H. petiolaris* subspecies to a homozygous inbred line of domesticated sunflower and genotyped the resulting F1 offspring. This test-cross design allows us to infer where recombination occurred in the heterozygous parents because we can reliably track the segregation of those parents' alleles against a predictable background (Figure 2).

Specifically, we used pollen from a single *H. petiolaris ssp. petiolaris* plant (PI435836) and a single *H. petiolaris ssp. fallax* plant (PI435768) to fertilize individuals of a highly inbred and male sterile line of *H. annuus* (HA89cms). The self-incompatible *H. petiolaris* accessions were collected in central Colorado (PI435836, 39.741°, −105.342°, Boulder County) and the southeast corner of New Mexico (PI435768, 32.3°, −104.0°, Eddy County; Figure S1), and were maintained at large population sizes by the US Department of Agriculture. When it was originally collected, accession PI435768 was classified as *H. neglectus*. However, based on the location of the collection (Heiser 1961) and a more recent genetic analysis of the scale of differences between *H. petiolaris* ssp. *fallax* and *H. neglectus* (Raduski *et al.* 2010), we believe that this accession should be classified *H. petiolaris ssp. fallax*.

### *Genotyping*

We collected leaf tissue from 116 *H. annuus* × *H. petiolaris* ssp. *petiolaris* F1 seedlings and 132 *H. annuus* × *H. petiolaris*

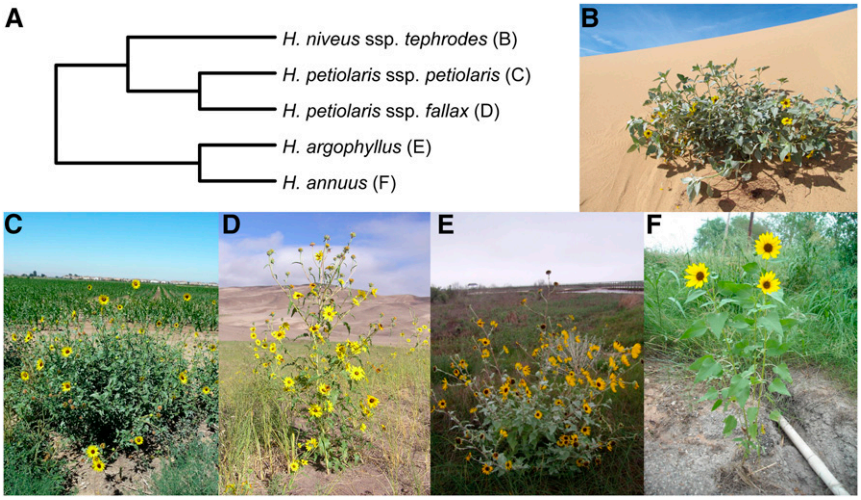


**Figure 1** The sunflower taxa used in this study. (A) Phylogenetic relationships based on Stephens *et al.* (2015) and Baute *et al.* (2016). (B) *H. niveus* ssp. *tephrodes*. (C) *H. petiolaris* ssp. *petiolaris*. (D) *H. petiolaris* ssp. *fallax*. (E) *H. argophyllus*. (F) *H. annuus*. Photo credits: Brook Moyers (B, C, E, and F) and Rose Andrew (D).

ssp. *fallax* F1 seedlings. We extracted DNA using a modified CTAB protocol (Doyle and Doyle 1987) and prepared individually barcoded genotyping-by-sequencing (GBS) libraries using a version of the Poland *et al.* (2012) protocol. Our modified protocol includes steps to reduce the frequency of high-copy fragments (*e.g.*, chloroplast and repetitive sequences) based on Shagina *et al.* (2010) and Matvienko *et al.* (2013), and steps to select specific fragment sizes for sequencing [see appendix B in Ostevik (2016) for the full protocol].

Briefly, we digested 100 ng of DNA from each individual with restriction enzymes (either *Pst*I-HF or *Pst*I-HF, and *Msp*I), and ligated individual barcodes and common adapters to the digested DNA. We pooled barcoded fragments from up to 192 individuals, cleaned and concentrated the libraries using SeraMag Speed Beads made in-house (Rohland and Reich 2012), and amplified fragments using 12 cycles of PCR. We depleted high-copy fragments based on Todesco *et al.* (2019) using the following steps: (1) denature the libraries using high temperatures, (2) allow the fragments to rehybridize, (3) digest the double-stranded fragments with duplex-specific nuclease (Zhulidov *et al.* 2004), and (4) amplify the undigested fragments using another 12 cycles of PCR. We ran the libraries out on a 1.5% agarose gel and extracted 300–800-bp fragments using a Zymoclean Gel DNA Recovery kit (Zymo Research, Irvine, CA). Then, following additional library cleanup and quality assessment, we sequenced paired ends of our libraries on an Illumina HiSeq 2000 (Illumina Inc., San Diego, CA).

To call variants, we used a pipeline that combines the Burrows–Wheeler Aligner version 0.7.15 (BWA) (Li and Durbin 2010) and the Genome Analysis Toolkit version 3.7 (GATK) (McKenna *et al.* 2010). First, we demultiplexed the data using sabre (Joshi 2011). Next, we aligned reads to the *H. annuus* reference (HanXRQr1.0-20151230; Badouin *et al.* 2017) with BWA-mem (Li 2013), called variants with GATK "HaplotypeCaller," and jointly genotyped all samples within a cross type with GATK "GentypeGVCFs." We split variants into SNPs and insertions/deletions (indels), and filtered each marker type using hard-filtration criteria suggested in the GATK best practices (DePristo *et al.* 2011; Van der Auwera *et al.* 2013). Specifically, we removed SNPs that had quality by depth scores (QD) $< 2$, strand bias scores (FS) $> 60$, mean mapping quality (MQ) $< 40$ or allele mapping bias scores (MQRankSum) $< -12.5$, and indels that had QD $< 2$ or FS $> 200$. After further filtering variants for biallelic and triallelic markers with genotype calls in at least 50% of individuals, we used GATK "VariantsToTable" to merge SNPs and indels into a single variant table for each cross type.

Finally, we converted our variant tables into AB format, such that the heterozygous parents contribute "A" and "B" alleles to offspring, while the *H. annuus* parent contributes exclusively A alleles. At biallelic markers (Figure 2A), sites with two reference alleles became "AA," and sites with the reference allele and the alternate allele became "AB." At triallelic markers (Figure 2B), sites with the reference allele and one alternate allele became AA, and sites with the reference allele and the other alternate allele became "AB." This method randomly assigns A and B alleles to the homologous chromosomes in each heterozygous parent, so our genetic maps initially consisted of pairs of mirror-imaged linkage groups that we later merged.

### *Genetic mapping*

We used R/qtl (Broman *et al.* 2003) in conjunction with R/ASMap (Taylor and Butler 2017) to build genetic maps. After excluding markers with $< 20\%$ or $> 80\%$ heterozygosity, and individuals with $< 50\%$ of markers scored, we used the function "mstmap.cross" with a stringent significance threshold ($P$-value $= 1 \times 10^{-16}$) to form conservative linkage groups. We used the function "plotRF" to identify pairs of linkage groups with unusually high recombination fractions and the function "switchAlleles" to reverse the genotype scores of one linkage group in each mirrored pair. We did this until reversing genotype scores no longer reduced the number of linkage groups.

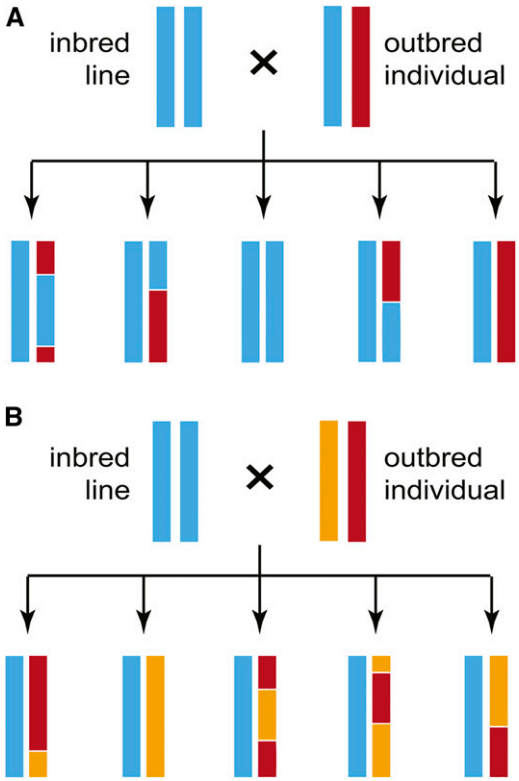


**Figure 2** Diagram showing how a test cross can be used to map the recombination events in an outbred individual that may (A) or may not (B) share alleles with the inbred line. Each line represents a chromosome, and the colors represent ancestry.

Using the corrected genotypes, we made new linkage groups with only the most reliable markers. Namely, we used the function "mstmap.cross" (with the parameter values: dist.fun = "kosambi", *P*-value = $1 \times 10^{-6}$, noMap.size = 2, and noMap.dist = 5) on markers with < 10% missing data and without significant segregation distortion. We refined the resulting linkage groups by removing: (1) markers with more than three double crossovers, (2) markers with aberrant segregation patterns (segregation distortion > 2 SD above or below the mean segregation distortion of the nearest 20 markers), and (3) linkage groups made up of less than four markers.

We progressively pushed markers with increasing amounts of segregation distortion and missing data into the maps using the function "pushCross." After adding each batch of markers, we reordered the linkage groups, and dropped markers and linkage groups as described above. Once all the markers had been pushed back, we used the function "calc.errorlod" to identify possible genotyping errors (error scores > 2) and replaced those genotypes with missing data. We continued to drop linkage groups, markers, and genotypes that did not meet our criteria until none remained.

Finally, we dropped five excess linkage groups, each made up of < 30 markers, from each map. The markers in these linkage groups mapped to regions of the *H. annuus* genome that were otherwise represented in the final genetic maps but could not be explained by reversed genotypes. Instead, these markers were likely polymorphic in the HA89cms individual used for crosses because of the 2–4% residual heterozygosity in sunflower inbred lines (Mandel *et al.* 2013).

### *Development of syntR*

To aid in the identification of chromosomal rearrangements, we developed the R package syntR (code and documentation available at http://ksamuk.github.io/syntR). This package implements a heuristic algorithm for systematically detecting synteny blocks from marker positions in two genetic maps. The key innovation of the syntR algorithm is coupling a biologically informed noise-reduction method with a cluster-identification method better suited for detecting linear (as opposed to circular) clusters of data points.

We based the syntR algorithm on the following statistical and biological properties of genetic maps and chromosomal rearrangements:

1. Synteny blocks appear as contiguous sets of orthologous markers in the same or reversed order in pairs of genetic maps (Pevzner and Tesler 2003; Choi *et al.* 2007).
2. The inferred order of markers in individual genetic maps is subject to error due to genotyping errors and missing data (Hackett and Broadfoot 2003). This error manifests as slight differences in the order of nearby markers within a linkage group between maps. This mapping error (which we denote "error rate one") results in uncertainty in the sequence of markers in synteny blocks.
3. In genomes with a history of duplication, seemingly orthologous markers can truly represent paralogs. These errors ("error rate two") look like tiny translocations and also disrupt marker orders within synteny blocks.
4. When comparing genetic maps derived from genomes without duplications or deletions, every region of each genome will be uniquely represented in the other. Because syntR is made for comparing homoploid genomes with this property, we expect each point in each genetic map to be contained within a single unique synteny block. Therefore, overlaps between synteny blocks are likely errors. Note that this assumption precludes the identification of duplications.
5. Chromosomal rearrangements can be of any size, but smaller rearrangements are difficult to distinguish from error (Pevzner and Tesler 2003). A key decision in synteny block detection is thus the choice of a detection threshold for small rearrangements, which results in a trade-off between error reduction and the minimum size of detectable synteny blocks.

The first step of the syntR algorithm is to smooth over mapping error (error rate one) by identifying highly localized clusters of markers based on a genetic distance threshold (cM) in both maps using hierarchical clustering (Figure 3A). The number of clusters formed is determined by the parameter maximum cluster range ($CR_{max}$) that defines the maximum genetic distance (cM) that any cluster can span in either

genetic map. After determining these initial clusters, we smooth the maps by collapsing each multimarker cluster down into a single representative point (the centroid of the cluster) for processing in subsequent steps. Next, we address errors introduced by poorly mapped or paralogous markers (error rate two) by flagging and removing outlier clusters that do not have a neighboring cluster within a specified maximum genetic distance (cM), a parameter we denote nearest neighbor distance ($NN_{dist}$, Figure 3B).

After the noise-reduction steps, we define preliminary synteny blocks using a method similar to the "friends-of-friends" clustering algorithm (Huchra and Geller 1982). First, we transform the genetic position of each cluster into rank order to minimize the impact of gaps between markers. We then group clusters that are: (1) adjacent in rank position in one of the maps and (2) within two rank positions in the other map (Figure S2). This grouping method further reduces the effect of mapping error by aggregating over pairs (but not triplets) of clusters that have reversed orientations. If a minimum number of clusters per synteny block has been (optionally) defined, we sequentially eliminate blocks that fall below the minimum number of clusters, starting with blocks made up of one cluster and ending with blocks made up of clusters equal to one less than the minimum. After each elimination, we regroup the clusters into new synteny blocks. Finally, we adjust the extents of each synteny block by removing overlapping sections from both synteny blocks so that every position in each genetic map is uniquely represented (Figure 3C).

### *Assessing the performance of the syntR algorithm*

To evaluate the performance of this method and explore the effect of parameter choice on outcomes, we simulated genetic map comparisons with known inversion breakpoints and error rates in R. The genetic map comparisons were made by randomly placing 200 markers at 100 positions along a 100-cM chromosome in two maps, reversing marker positions within a defined inversion region in one map, and then repositioning markers based on simulated mapping noise using the following two error parameters: (1) $ER_1$ is the SD of a normal distribution used to pick the distances markers are pushed out of their correct positions (*e.g.*, when $ER_1$ is 1 cM, 95% of markers will be within 2 cM of their true position) and (2) $ER_2$ is the proportion of markers that are repositioned according to a uniform distribution (*i.e.*, these markers can be moved to any position on the simulated chromosome).

We initially ran syntR using fixed syntR parameters ($CR_{max}$ = 2 and $NN_{dist}$ = 10) on multiple simulated maps, which were made using variable parameters (inversion size: 2.5–50 cM, $ER_1$: 0–2.0 cM, and $ER_2$: 0–20%), and counted the number of times the known breakpoints were identified within 1 cM (Figure S3). As expected, we find that rearrangement size affects the false-negative rate (*i.e.*, failing to detect known breakpoints), such that smaller inversions are more likely to be missed (Figure S3C), but does not affect the false-positive rate (*i.e.*, detecting breakpoints where there are none). We also find that increasing both types of error in the genetic maps tends to increase both the false-positive and false-negative rates, although $ER_1$ has a much stronger effect on the false-positive rate than any other combination (Figure S3, A and B).

Using the same simulation methods as above but now varying the syntR parameter $CR_{max}$, we find that small values of $CR_{max}$ yield high false-positive rates while large values yield high false-negative rates (Figure S4A). In addition, the $ER_1$ parameter has a strong effect on the relationship between $CR_{max}$ and the false-positive rate. Higher values of $CR_{max}$ are needed to reduce the false-positive rate when $ER_1$ is also high (Figure S4B). This means that picking an appropriate $CR_{max}$ value is key to the accuracy of this method. Although $NN_{dist}$ has a much weaker effect on outcomes than $CR_{max}$, it is useful to consider both parameter values carefully.

When the syntR heuristic algorithm is performing well, the final synteny blocks should represent all positions in the two genetic maps being compared (Chen *et al.* 2009). Based on this characteristic, we developed a method to choose optimal syntR tuning parameters ($CR_{max}$ and $NN_{dist}$) that maximize the representation of the genetic maps and markers in synteny blocks. In this method a user: (1) runs syntR with a range of parameter combinations, (2) saves summary statistics about the genetic distance of each map represented in the synteny blocks and the number of markers retained for each run, and (3) finds the parameter combination that maximizes a composite statistic that equally weights these three measures. In cases where there are multiple local maxima, we suggest choosing the local maximum with the smallest value of $CR_{max}$ to reduce the number of potential false positives.

The "maximize representation" method for choosing syntR parameters has several benefits. First, it does not rely on any additional information (*e.g.*, error rate estimates from the genetic maps compared). Second, when we use this method to choose the best parameters for simulated genetic maps, we find that these parameter values also minimize false-positive and false-negative rates (Figure S5). Third, when we simulate biologically realistic genetic map comparisons, the absolute values of false positives and false negatives are small. For example, when comparing two genetic maps in which ~95% of markers are within 1 cM of their true position ($ER_1$ = 0.5) and 5% of markers are randomly permuted ($ER_2$ = 0.05), nonexistent breakpoints will be identified 0.1 times and a breakpoint of a 20 cM inversion will be missed 0.04 times. These low error rates also highlight the overall robustness and accuracy of the syntR algorithm.

In addition to performing simulations, we compared the synteny blocks identified by syntR to those identified by other means in a previously published comparison of *H. niveus* ssp. *tephrodes* and *H. argophyllus* maps to *H. annuus* (Barb *et al.* 2014). To do this, we formatted the original data sets for input into syntR and used the "maximize representation" method to determine the optimal parameter values for the two comparisons (*H. niveus vs. H. annuus*: $CR_{max}$ = 1.5, $NN_{dist}$ = 30; *H. argophyllus vs. H. annuus*: $CR_{max}$ = 2, $NN_{dist}$ = 20). We found that syntR was in strong agreement with previous work (Figure S6), recovering all the same

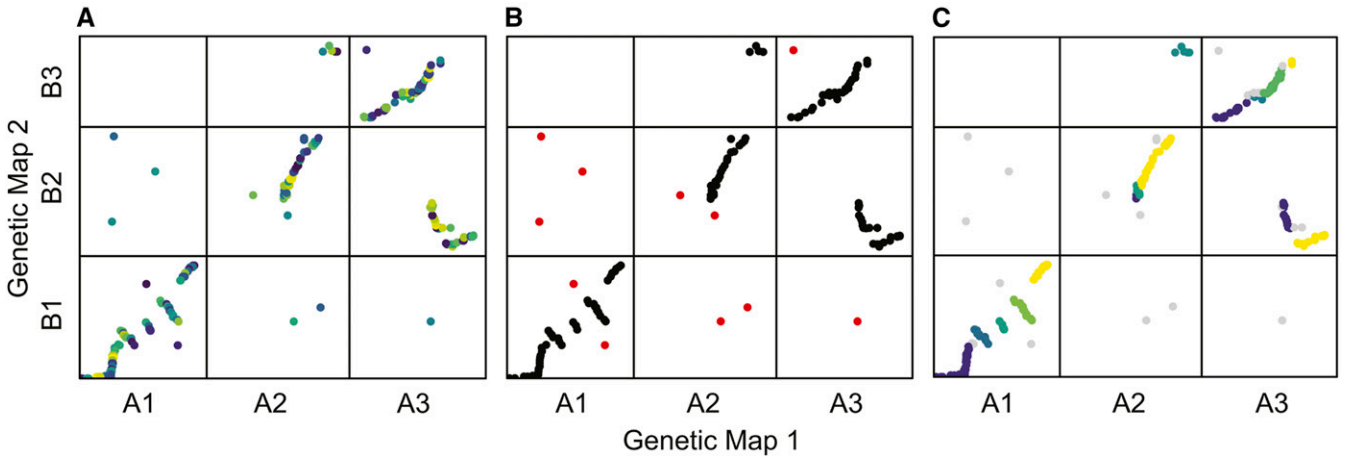


**Figure 3** The stages of the syntR algorithm. Each plot shows the relationship between markers or clusters of markers from three chromosomes in two genetic maps. (A) Highly localized markers are clustered. Each shade represents an individual cluster of markers that will be collapsed into a single representative point. (B) Clusters without another cluster nearby are dropped. Red points represent clusters without a neighbor within 10 cM. (C) Clusters are grouped into synteny blocks based on their rank positions. Gray points represent markers that were dropped in previous steps, and each other color represents a different synteny block.

translocations and most of the same inversions as the Barb *et al.* (2014) maps. Most of the cases of mismatches were very small or weakly supported inversions in the Barb *et al.* (2014) maps that syntR did not identify.

### *Finding synteny blocks*

We used syntR to identify synteny blocks between our newly generated genetic maps and an ultrahigh-density map of *H. annuus* that was used to build the sunflower genome that we used as a reference (Badouin *et al.* 2017). This allowed us to easily convert between physical position in the *H. annuus* reference and position in the *H. annuus* genetic map. Using this property, we further compared two previously published genetic maps for the closely related sunflower species, *H. niveus* ssp. *tephrodes* and *H. argophyllus* (Barb *et al.* 2014), to the same *H. annuus* map. We aligned marker sequences from the published maps to the *H. annuus* reference using BWA and converted well-aligned markers (MQ $>$ 40) to their positions in the *H. annuus* genetic map.

Initially, we ran syntR using parameters identified through the "maximize representation" method for each map comparison separately (Table S1). However, varying $CR_{max}$ revealed rearrangements that were shared between the maps (Figure S7). Therefore, we ran syntR again using a range of $CR_{max}$ values that included the best fit for each comparison (1.0–3.5 in 0.5 increments) and extracted a curated set of synteny blocks from the output. A synteny block was retained if it fulfilled any of the following criteria (in decreasing order of importance): (1) it was found in another species, (2) it was identified in the majority of syntR runs for a single species, and (3) it maximized the genetic distance represented by synteny blocks. We present this curated set of synteny blocks below, but our results are unchanged if we use the individually fitted synteny blocks.

We named the chromosomes in our genetic maps based on their synteny with the standard order and orientation of *H. annuus* chromosomes (Tang *et al.* 2002; Bowers *et al.* 2012) following Barb *et al.* (2014) but with shortened prefixes (A = *H. annuus*, R = *H. argophyllus*, N = *H. niveus* ssp. *tephrodes*, *P* = *H. petiolaris* ssp. *petiolaris*, and F = *H. petiolaris* ssp. *fallax*). For example, an *H. petiolaris* ssp. *fallax* chromosome made up of regions that are syntenic with *H. annuus* chromosomes 4 and 7 is called F4–7.

### *Karyotype reconstruction and analysis*

We used our inferred synteny blocks and the software MGR v 2.01 (Bourque and Pevzner 2002) to infer ancestral karyotypes for our five *Helianthus* taxa and to determine the number of chromosomal rearrangements that occurred along each branch of the species tree. To run the MGR analysis, we needed the order and orientations of synteny blocks in all five maps. However, individual synteny blocks were often missing from one or more of our final maps. We approached this problem in two ways. First, we inferred the likely position of missing synteny blocks based on the location of markers that were too sparse to be grouped by syntR and matched the location of synteny blocks in other maps. In the second case, we dropped any synteny blocks that were not universally represented. Because we already had two sets of synteny blocks for each map (curated and individually optimized), we ran the MGR analyses using three different sets of synteny blocks: set 1 (curated and inferred), set 2 (curated and present in all five maps), and set 3 (individually optimized and present in all five maps).

### *Data availability*

The R program, syntR, is available on GitHub: https://github.com/ksamuk/syntR. The sequences used to generate genetic maps are available at the Sequence Read Archive: http://www.ncbi.nlm.nih.gov/bioproject/598366. All other

data and scripts are available on dryad: https://doi.org/10.5061/dryad.7sqv9s4pc. Supplemental material available at figshare: https://doi.org/10.25386/genetics.11819625.

## Results

### Genetic maps

Both *H. petiolaris* genetic maps are made up of the expected 17 chromosomes and have very high marker densities (Figure 4 and Figure S8). Only 6% of the *H. petiolaris* ssp. *petiolaris* map and 10% of the *H. petiolaris* ssp. *fallax* map fails to have a marker within 2 cM (Figure S9). Overall, both maps are somewhat longer than the *H. petiolaris* map reported by Burke *et al.* (2004). Although this could represent real variation between genotypes, it could also be the result of spurious crossovers that are inferred based on genotyping errors. Because genotyping errors are proportional to the number of markers, maps with high marker densities are more likely to be inflated. Indeed, building maps with variants that are thinned to 1 per 150 bp using vcftools version 0.1.13 (Danecek *et al.* 2011) yields collinear maps that are closer to the expected lengths (Figure S10 and Table S2,). We present subsequent results based on the full maps to improve our resolution for detecting small rearrangements.

Despite the general expansion of our maps, we find that chromosomes 2 and 4 in the *H. petiolaris* ssp. *fallax* map (F2 and F4) are unexpectedly short (Figure 4). When we look at the distribution of markers for this map relative to the *H. annuus* reference, we find very few variable sites in the distal half of these chromosomes (Figure S11). That is, this individual was homozygous along vast stretches of F2 and F4. These runs of homozygosity could be explained by recent common ancestry (*i.e.*, inbreeding) or a lack of variation in the population (*e.g.*, because of background selection or a recent selective sweep). Regardless, the lack of variable sites within the *H. petiolaris* ssp. *fallax* individual used for crosses explains the shortness of F2 and F4. Notably, we find the same pattern on the distal half of *H. annuus* chromosome 7 and find that this region is also not represented in the *H. petiolaris* spp. *fallax* map.

### Synteny blocks

Using syntR, we recovered 97 genetic regions that are syntenic between *H. petiolaris* ssp. *petiolaris* and *H. annuus*, and 79 genetic regions that are syntenic between *H. petiolaris* ssp. *fallax* and *H. annuus* (Figure 4). We also recovered synteny blocks for the *H. niveus* ssp. *tephrodes* and *H. argophyllus* comparisons that are similar to those found previously (Figure S13). In all four comparisons, syntR successfully identified synteny blocks that cover large proportions (63–90%) of each genetic map, even in the face of a very high proportion of markers that map to a different chromosome than their neighbors (Table 1). These "rogue markers" could be the result of very small translocations, poorly mapped markers, or extensive paralogy. Over and above the prevalence of rogue markers, the karyotypes we recovered are substantially rearranged. Only between 32% and 45% of synteny blocks for each map are collinear with the *H. annuus* genetic map in direct comparisons (Table 1).

### Karyotype reconstruction and chromosomal rearrangement

Because nested and shared rearrangements can obscure patterns of chromosome evolution, we use the MGR analyses to predict the most likely sequence of rearrangements in a phylogenetic context before quantifying the rearrangement rate. These MGR analyses identified similar patterns of chromosome evolution regardless of the exact set of synteny blocks that we used (Table S5). Multiple taxa share many rearrangements, and the similarity of karyotypes matches known phylogenetic relationships. Moreover, MGR analyses run without a guide tree inferred the known species tree, and MGR analyses run with all other topologies identified an inflated number of chromosomal rearrangements.

Using the most complete set of synteny blocks (set 1), we find that 88 chromosomal rearrangements occurred across the phylogeny (Figure 5). Then, using the most current divergence time estimates for this group (Todesco *et al.* 2019) and conservatively assuming that *H. niveus* ssp. *tephrodes* diverged at the earliest possible point, we estimate that 7.9 (7.8–8) rearrangements occurred per million years in this clade (Tables S3–S5). To further explore the potential range of rearrangement rates, we considered other estimates of divergence times in sunflower (Sambatti *et al.* 2012; Mason 2018) and the other sets of synteny blocks. Overall, the lowest rate we identified was 2.6 rearrangements per million years, while the highest rate was indeterminable because some minimum divergence time estimates for the group include 0 (Tables S3–S5).

The 88 rearrangements include 74 inversions and 14 translocations that are quite evenly distributed across the phylogeny. However, the excess inversions indicate that it is unlikely that the rate of inversions is equal to the rate of translocation (binomial test, $5.1 \times 10^{-11}$). Furthermore, we find that only 8 of the 17 chromosomes are involved in the 14 translocations we identified. If translocations were equally likely for all chromosomes, this asymmetry would be very unlikely to have happened by chance (the probability of sampling at most eight chromosomes in 14 translocations is $8.0 \times 10^{-8}$, Figure S15), suggesting that some chromosomes are more likely to be involved in translocations than other. In line with this observation, we see that some chromosome segments are repeatedly translocated. For example, A4 and A7 are involved in several exchanges, and part of A6 has a different position in almost every map (Figure 5).

## Discussion

Large-scale chromosomal changes may be key contributors to the process of adaptation and speciation, yet we still have a poor understanding of rates of chromosomal rearrangement and the evolutionary forces underlying those rates. Here, we

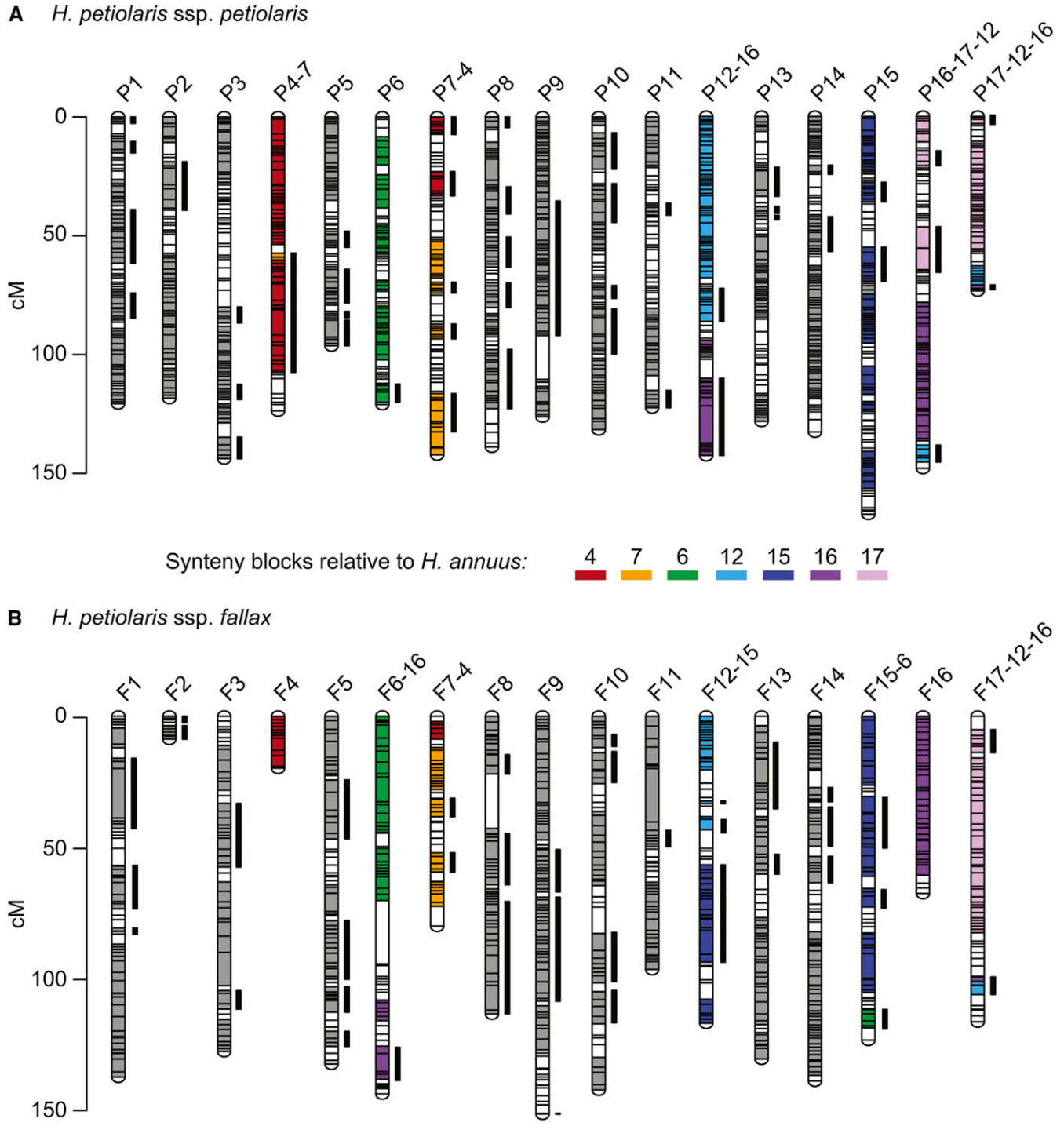


**Figure 4** H. *petiolaris* genetic maps showing blocks of synteny with *H. annuus*. Each horizontal bar represents a genetic marker. The thick vertical bars next to chromosomes represent synteny blocks that are inverted relative to the *H. annuus* genetic map. Where there are no translocations between *H. petiolaris* and *H. annuus* chromosomes (*e.g.*, all synteny blocks in P1 and F1 are syntenic with A1), the synteny blocks are shown in gray. Where there are translocations, the synteny blocks are color-coded based on their synteny with *H. annuus* chromosomes. Regions that are not assigned to a synteny block remain white. The synteny blocks plotted are those curated based on multiple runs of syntR using different parameters. Please see Figure S12 for a labeled version. This figure was made with LinkageMapView (Ouellette *et al.* 2017).

devised a novel, systematic method for comparing any pair of genetic maps, and performed a comprehensive analysis of the evolution of chromosomal rearrangements in a clade of sunflowers. We created two new genetic maps for *Helianthus* species and used our new method to identify a wide range of karyotypic variation in our new maps, as well as previously published maps. Consistent with previous studies, we discovered a high rate of chromosomal evolution in the annual

**Table 1 Properties of the synteny blocks found using a syntR analysis between genetic maps of *H. annuus* and four other *Helianthus* taxa**

| Genetic map | Number of synteny blocks | Rogue markers (%) | Map coverage | *H. annuus* coverage | Collinear | Inverted | Translocated |
|---|---|---|---|---|---|---|---|
| *H. petiolaris* ssp. *petiolaris* | 97 | 19 | 80% | 74% | 39% | 36% | 26% |
| *H. petiolaris* spp. *fallax* | 79 | 17 | 63% | 65% | 32% | 34% | 34% |
| *H. niveus* ssp. *tephrodes* | 43 | 26 | 78% | 75% | 40% | 21% | 39% |
| *H. argophyllus* | 31 | 20 | 90% | 82% | 45% | 16% | 39% |

The proportion of rogue markers is based only on the chromosomes without translocations in any map (*i.e.*, chromosomes 1–3, 5, 8–10, 11, and 14). For those chromosomes, the majority of markers mapped to a single *H. annuus* chromosome. The other markers are considered rogue.

sunflowers. Further, we found that inversions are more common than translocations and that certain chromosomes are more likely to be translocated. Below, we discuss the evolutionary and methodological implications of this work and suggest some next steps in understanding the dynamic process of chromosomal rearrangement.

### *Identifying rearrangements*

Studying the evolution of chromosomal rearrangements requires dense genetic maps and systematic methods to analyze and compare these maps between species. Our new software, syntR, provides an end-to-end solution for systematic and repeatable identification of synteny blocks in pairs of genetic maps with any marker density. Our tests on real and simulated data find that syntR recovers chromosomal rearrangements identified previously by both manual comparisons and cytological studies, suggesting that syntR is providing an accurate view of karyotypic differences between species.

Overall, we believe that syntR will be a valuable tool for the systematic study of chromosomal rearrangements in any species. The only data syntR needs to identify synteny blocks is relative marker positions in two genetic maps. This fact is significant because, although the number of species with whole-genome sequences and methods to detect synteny blocks from those sequences are rapidly accumulating, such as Mauve (Darling *et al.* 2004), Cinteny (Sinha and Meller 2007), syMAP (Soderlund *et al.* 2011), SynChro (Drillon *et al.* 2014), and SyRI (Goel *et al.* 2019), it is still uncommon to have multiple closely related whole-genome sequences that are of sufficient quality to compare for karyotype differences. At the same time, the proliferation of reduced-representation genome sequencing methods means that it is easy to generate many genetic markers for nonmodel species and produce very dense genetic maps. Furthermore, syntR allows comparisons to include older genetic map data that would otherwise go unused. The simplicity of the syntR algorithm will facilitate rapid karyotype mapping in a wide range of taxa.

We also believe that syntR provides a baseline for the development of further computational and statistical methods for the study of chromosomal rearrangements. One fruitful direction would be to integrate the syntR algorithm for synteny block detection directly into the genetic map-building process (much like GOOGA; Flagel *et al.* 2019). Another key extension would be to allow syntR to compare multiple genetic maps simultaneously to detect synteny blocks in a group of species (*e.g.*, by leveraging information across species). Finally, formal statistical methods for evaluating the model fit and the uncertainty involved with any set of synteny blocks would be a major (albeit challenging) improvement to all existing methods, including syntR.

### *The similarity of H. petiolaris maps to previous studies*

Compared with previous work, we found more inversions and fewer translocations between *H. petiolaris* subspecies and *H. annuus* (Rieseberg *et al.* 1995; Burke *et al.* 2004). This is probably due to a combination of factors. First, there appears to be karyotypic variation within some *Helianthus* species (Heiser 1948, 1961; Chandler *et al.* 1986). Second, the maps presented here are made up of more markers and individuals, which allowed us to identify small inversions that were previously undetected as well as to eliminate false linkages that can be problematic in small mapping populations. Lastly, we required more evidence to call rearrangements. Although we recovered some of the translocations supported by multiple markers in Rieseberg *et al.* (1995) and Burke *et al.* (2004), we did not recover any of the translocations supported by only a single sequence-based marker. Given the high proportion of rogue markers in our maps, it is likely that some of the putative translocations recovered in those earlier comparisons are the result of the same phenomenon.

On the other hand, we found that rearrangements between our *H. petiolaris* maps match the translocations predicted from cytological studies quite well. Heiser (1961) predicted that *H. petiolaris* ssp. *petiolaris* and *H. petiolaris* ssp. *fallax* karyotypes would have three chromosomes involved in two translocations that form a ring during pairing at meiosis, as well as the possibility of a second independent rearrangement. This exact configuration is likely to occur at meiosis in hybrids between the *H. petiolaris* subspecies maps we present here (Figure S16). Also, the most noteworthy chromosome configuration in cytological studies of *H. annuus–H. petiolaris* hybrids (Heiser 1947; Whelan 1979; Ferriera 1980; Chandler *et al.* 1986) was a hexavalent (a six-chromosome structure) plus a quadrivalent (a four-chromosome structure). Again, this is the configuration that we would expect in a hybrid between *H. annuus* and the *H. petiolaris* ssp. *petiolaris* individual mapped here. Furthermore, the complicated arrangement and relatively small sizes of A12, A16, and A17 synteny blocks in *H. petiolaris* might explain

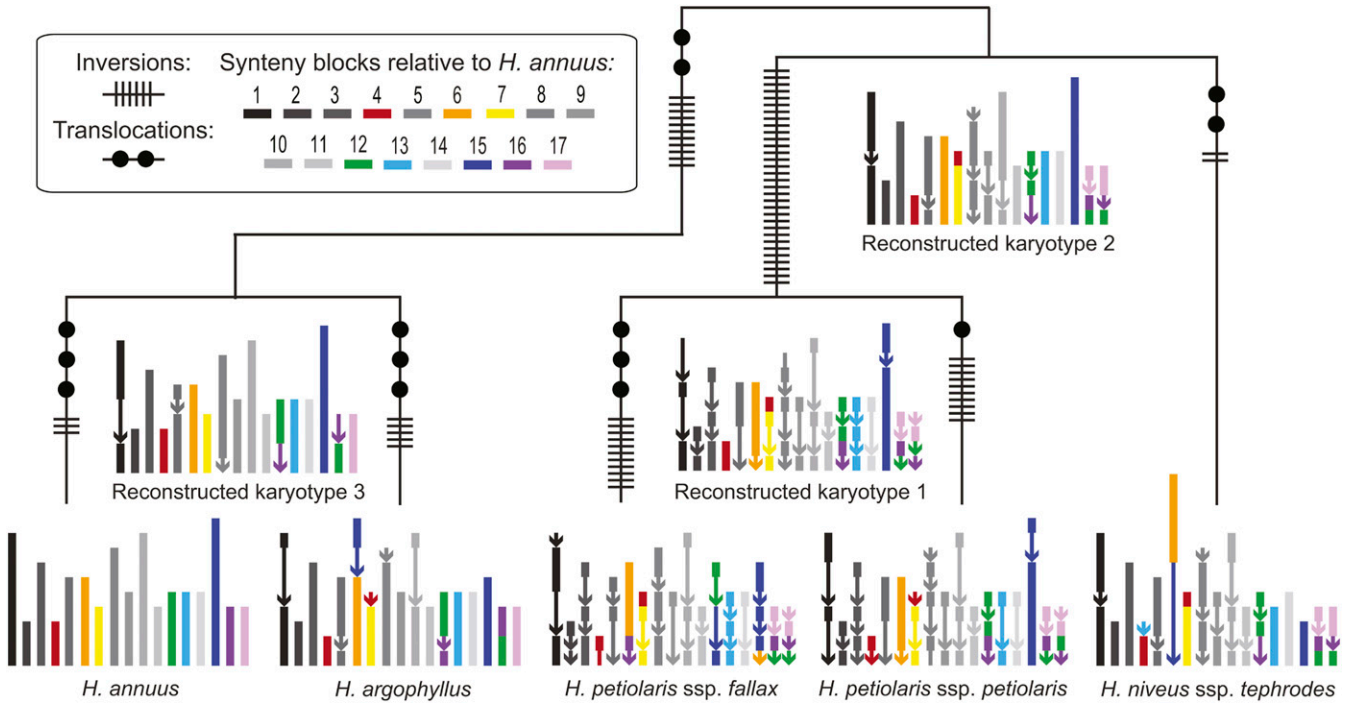


**Figure 5** Diagram showing the karyotypes of five *Helianthus* taxa as well as reconstructed ancestral karyotypes and the locations of chromosomal rearrangements. The karyotypes were built using synteny block set 1, and were curated based on multiple syntR runs and inferred when missing. Each synteny block is represented using a line segment that is color-coded based on its position in the *H. annuus* genome (see Figure S14 for a labeled version). Chromosomes without translocations in any map are plotted in gray, and synteny blocks that are inverted relative to *H. annuus* are plotted using arrows. Also, note that along some branches the same pair of chromosomes is involved in multiple translocations.

why cytological configurations in *H. annuus–H. petiolaris* hybrids are so variable. Interestingly, the rearrangements identified between *H. argophyllus* and *H. annuus* karyotypes here and in Barb *et al.* (2014) also match the cytological studies better than an earlier comparison of sparse genetic maps (Heesacker *et al.* 2009). It seems that, in systems with the potential for high proportions of rogue markers, many markers are needed to identify chromosomal rearrangements reliably.

### *Total rearrangement rates*

Our data suggest that annual sunflowers experience ~7.9 chromosomal rearrangements per million years. This rate overlaps with recent estimates for this group (7.4–10.3, Barb *et al.* 2014) and is even higher than the estimate that highlighted sunflower as a group with exceptionally fast chromosomal evolution (5.5–7.3, Burke *et al.* 2004). However, since Burke *et al.* (2004), chromosomal rearrangements have been tracked in many additional groups, including mammals (Ferguson-Smith and Trifonov 2007; Martinez *et al.* 2016; Oliveira da Silva *et al.* 2019), fish (Molina *et al.* 2014; Ayres-Alves *et al.* 2017), insects (Rueppell *et al.* 2016; Corbett-Detig *et al.* 2019), fungi (Sun *et al.* 2017), and plants (Yogeeswaran *et al.* 2005; Schranz *et al.* 2006; Huang *et al.* 2009; International Brachypodium Initiative 2010; Latta *et al.* 2019). Of these analyses, relatively few have systematically studied karyotype evolution across multiple species and estimated total rearrangement rates. Of those that do, most studies report <7.9 chromosomal rearrangements per million years, for example, in *Solanum* (0.36–1.44; Wu and Tanksley 2010), *Drosophila* (0.44–2.74; Bhutkar *et al.* 2008), and mammals (0.05–2.76; Murphy *et al.* 2005). However, there are exceptions, such as a comparison of genome sequences that revealed up to 35.7 rearrangements per million years in some grass lineages (Dvorak *et al.* 2018).

At the same time, we are likely underestimating rearrangement rates here for two reasons. First, we used conservative thresholds for calling rearrangements. For example, some proportion of the rogue markers that we identified could be the result of very small but real chromosomal rearrangements. Second, our ability to resolve very small synteny blocks and breakpoints between synteny blocks depends on marker density. Until we have full genome sequences to compare (like for the grass lineages), we could be failing to detect very small rearrangements and falsely inferring that independent rearrangements are shared. However, regardless of just how much we are underestimating the rate, sunflower chromosomes are evolving quickly. This high rate of chromosomal evolution could be a consequence of a higher rate of chromosomal mutation, a decreased chance that chromosomal polymorphisms are lost, or both processes.

### *Type of rearrangements*

We found that inversions and interchromosomal translocations dominate chromosomal evolution in *Helianthus*. This

pattern is common in angiosperm lineages (Weiss-Schneeweiss and Schneeweiss 2012) and fits with the consistent chromosome counts across annual sunflowers ($2n = 34$; Chandler *et al.* 1986). In addition, we found more inversions than translocations, which has previously been seen in both plant (Wu and Tanksley 2010; Amores *et al.* 2014) and animal systems (Rueppell *et al.* 2016), and echoes general reports that intrachromosomal rearrangements are more common than interchromosomal rearrangements (Pevzner and Tesler 2003). These consistent rate differences are notable because, although both rearrangement types depend on double-strand breaks, two of the major consequences of chromosomal rearrangements, underdominance (*i.e.*, rearrangement heterozygotes are less fit than either homozygote) and recombination modification, might be more common for some types of rearrangements.

Translocations have a more predictable effect on hybrid fertility, while inversions consistently reduce recombination. Reciprocal translocation heterozygotes can affect fertility because missegregation during meiosis can cause one-half of the gametes to be unbalanced and thus inviable (White 1973; King 1993). Although inversion heterozygotes can also produce unbalanced gametes, whether that happens is dependent on the size of the inversion and whether disrupted pairing during meiosis inhibits crossovers (Searle 1993). When inversions are small or have suppressed crossing over, they will not be strongly underdominant. On the other hand, inversions often exhibit reduced recombination, either because recombination is suppressed through disrupted pairing (Searle 1993) or ineffective through the production of inviable gametes (Rieseberg 2001). While interactions between reduced recombination and adaptation with gene flow have been extensively examined in the case of inversions (Kirkpatrick and Barton 2006; Hoffmann and Rieseberg 2008; Yeaman and Whitlock 2011; Yeaman 2013), it is not clear whether the same pattern will be common for translocations [but see Fishman *et al.* (2013) and Stathos and Fishman (2014) for one example]. Translocations bring together previously unlinked alleles and mispairing at translocation breakpoints could suppress crossing over, but recombination inside reciprocal translocations will not necessarily produce inviable gametes and thus reduce effective recombination.

Although any selective force could be responsible for the evolution of any chromosomal rearrangement, potential differences in the relative magnitude of underdominance *vs.* recombination suppression may contribute to the evolution of sunflower chromosomes. While many chromosomal rearrangements in sunflowers appear to be strongly underdominant (Chandler *et al.* 1986, Lai *et al.* 2005), inversions typically are not (L. Rieseberg, unpublished data). If translocations tend to be more underdominant than inversions, they would be less likely to evolve through drift and more likely to cause reproductive isolation directly. This could explain why translocations are less common than inversions and why pollen viability is accurately predicted by the number of translocations inferred from cytological studies (Chandler *et al.* 1986). At the same time, recent genomic analyses have identified several extensive regions of very low recombination caused by large inversions segregating in natural sunflower populations (Todesco *et al.* 2019; Huang *et al.* 2019). Mutations that segregate for extended periods are unlikely to be strongly underdominant and these inversions are associated with multiple adaptive alleles (Todesco *et al.* 2019), which is consistent with a role for selection in their origin or maintenance.

### *Nonrandom chromosomal rearrangement*

We also found that some sunflower chromosomes are involved in more translocations than others. This pattern has been observed in wheat (Badaeva *et al.* 2007) and breakpoint reuse is a common phenomenon in comparative studies of karyotypes (Pevzner and Tesler 2003; Bailey *et al.* 2004; Murphy *et al.* 2005; Larkin *et al.* 2009). Many studies support the idea that chromosomal regions with greater sequence similarity are more likely to recombine and thus potentially generate novel chromosomal arrangements. Some of the clearest examples of this come from the polyploidy literature, where chromosomes with ancestral homology are more likely to recombine (Nicolas *et al.* 2007; Marone *et al.* 2012; Mason *et al.* 2014; Tennessen *et al.* 2014; Nguepjop *et al.* 2016). However, centromeres and other repetitive regions can also affect the rate of mutations that cause chromosomal rearrangements (Hardison *et al.* 2003; Murphy *et al.* 2005; Raskina *et al.* 2008; Molnár *et al.* 2010; Vitte *et al.* 2014; Ayers-Alves *et al.* 2017; Li *et al.* 2017; Corbett-Detig *et al.* 2019). Given that sunflowers have several genome duplications and a burst of transposable element activity in their evolutionary history (Barker *et al.* 2008, 2016; Kawakami *et al.* 2011; Staton *et al.* 2012; Badouin *et al.* 2017), it is plausible that ancestral homology or repeat content could be associated with translocation propensity.

Of the above possibilities, an association between repeated translocations and centromeres would be particularly compelling. Beyond the repeat content of centromeres explaining nonrandom mutation [Kawabe *et al.* (2006) and Sun *et al.* (2017), but see Lin *et al.* (2018) and Okita *et al.* (2019)], the positions and sizes of centromeres on chromosomes are known to affect meiotic drive, and thus the repositioning of centromeres through rearrangement could cause nonrandom fixation of translocations (Kaszás and Birchler 1998, Chmátal *et al.* 2014; Zanders *et al.* 2014). The relative placement of centromeres has been associated with chromosome evolution in *Brassica* (Schranz *et al.* 2006) and wheat (Badaeva *et al.* 2007), and associations between meiotic drive and chromosome evolution have been found in several animal taxa (Bidau and Martí 2004; Palestis *et al.* 2004; Molina *et al.* 2014; Blackmon *et al.* 2019). In sunflower, we see some hints that centromeric repeats might be associated with repeated translocation. Using the locations of the centromere-specific retrotransposon sequence HaCEN-LINE (Nagaki *et al.* 2015) to roughly identify the locations of centromeres in our reference, we find that some rearrangement breakpoints, *e.g.*, the

section of A16 with a different position in each map, are close to putative centromeres (Figure S17–S20). Although a more thorough analysis of centromeric repeat locations and their association with rearrangement breakpoints is required to draw firm conclusions about the importance of centromeres to chromosomal evolution in sunflower, the development of reference sequences for wild sunflower species is underway, which will allow those and other associations to be confirmed. Further, it is time to directly test for meiotic drive in this system by examining the transmission of rearrangements that affect centromeres in gametes produced by plants that have heterozygous karyotypes.

### *Conclusion*

Understanding the evolution of chromosomal rearrangements remains a key challenge in evolutionary genetics. By developing new software to systematically detect synteny blocks and building new genetic maps, we show that sunflowers exhibit rapid and nonrandom patterns of chromosomal evolution. These data generate specific and testable hypotheses about chromosomal evolution in sunflower. We believe that our work will spur additional studies of karyotypic evolution and diversity, and ultimately lead to a more comprehensive understanding of the interplay between chromosomal evolution and speciation.

## Acknowledgments

We thank Jessica Barb for providing marker sequence data; Marcy Uyenoyama for help with our random walk analysis; Greg Baute for sharing hybrid seed; Chris Grassa for growing seedlings and sharing scripts; Marco Todesco and Nadia Chaidir for help in the laboratory; and Jenn Coughlan, Andrew MacDonald, Brook Moyers, Mariano Alvarez, Dolph Schluter, Darren Irwin, Sally Otto, and three anonymous reviewers for thoughtful discussions and help with earlier drafts of this manuscript. This work was supported by an Natural Sciences and Engineering Research Council (NSERC) of Canada Postgraduate Scholarship awarded to K.L.O. and an NSERC Discovery grant awarded to L.H.R. (327475).

Author contributions: K.L.O. and L.H.R. planned the study. K.L.O. and K.S. designed and built the R package syntR. K.L.O. made genetic maps, carried out data analysis, and drafted the manuscript. All authors read, edited, and approved the final manuscript.

## Literature Cited

Amores, A., J. Catchen, I. Nanda, W. Warren, R. Walter *et al.*, 2014 A RAD-tag genetic map for the platyfish (*Xiphophorus maculatus*) reveals mechanisms of karyotype evolution among teleost fish. Genetics 197: 625–641. https://doi.org/10.1534/genetics.114.164293

Ayres-Alves, T., A. L. Cardoso, C. Y. Nagamachi, L. M. de Sousa, J. C. Pieczarka *et al.*, 2017 Karyotypic evolution and chromosomal organization of repetitive DNA sequences in species of *Panaque*, *Panaqolus*, and *Scobinancistrus* (Siluriformes and Loricariidae) from the Amazon Basin. Zebrafish 14: 251–260. https://doi.org/10.1089/zeb.2016.1373

Badaeva, E. D., O. S. Dedkova, G. Gay, V. A. Pukhalskyi, A. V. Zelenin *et al.*, 2007 Chromosomal rearrangements in wheat: their types and distribution. Genome 50: 907–926. https://doi.org/10.1139/G07-072

Badouin, H., J. Gouzy, C. J. Grassa, F. Murat, S. E. Staton *et al.*, 2017 The sunflower genome provides insights into oil metabolism, flowering and Asterid evolution. Nature 546: 148–152. https://doi.org/10.1038/nature22380

Bailey, J. A., R. Baertsch, W. J. Kent, D. Haussler, and E. E. Eichler, 2004 Hotspots of mammalian chromosomal evolution. Genome Biol. 5: R23. https://doi.org/10.1186/gb-2004-5-4-r23

Barb, J. G., J. E. Bowers, S. Renaut, J. I. Rey, S. J. Knapp *et al.*, 2014 Chromosomal evolution and patterns of introgression in *Helianthus*. Genetics 197: 969–979. https://doi.org/10.1534/genetics.114.165548

Barker, M. S., N. C. Kane, M. Matvienko, A. Kozik, R. W. Michelmore *et al.*, 2008 Multiple paleopolyploidizations during the evolution of the Compositae reveal parallel patterns of duplicate gene retention after millions of years. Mol. Biol. Evol. 25: 2445–2455. https://doi.org/10.1093/molbev/msn187

Barker, M. S., Z. Li, T. I. Kidder, C. R. Reardon, Z. Lai *et al.*, 2016 Most Compositae (Asteraceae) are descendants of a paleohexaploid and all share a paleotetraploid ancestor with the Calyceraceae. Am. J. Bot. 103: 1203–1211. https://doi.org/10.3732/ajb.1600113

Baute, G. J., G. L. Owens, D. G. Bock, and L. H. Rieseberg, 2016 Genome-wide genotyping-by-sequencing data provide a high-resolution view of wild Helianthus diversity, genetic structure, and interspecies gene flow. Am. J. Bot. 103: 2170–2177. https://doi.org/10.3732/ajb.1600295

Berdan E. L., G. M. Kozak, R. Ming, A. L. Rayburn, R. Kiehart *et al.*, 2014 Insight into genomic changes accompanying divergence: genetic linkage maps and synteny of *Lucania goodei* and *L. parva* reveal a Robertsonian fusion. G3 (Bethesda) 4: 1363–1372. https://doi.org/10.1534/g3.114.012096

Bhutkar, A., S. W. Schaeffer, S. M. Russo, M. Xu, T. F. Smith *et al.*, 2008 Chromosomal rearrangement inferred from comparisons of 12 *Drosophila* genomes. Genetics 179: 1657–1680. https://doi.org/10.1534/genetics.107.086108

Bidau, C. J., and D. A. Martí, 2004 B chromosomes and Robertsonian fusions of *Dichroplus pratensis* (Acrididae): intraspecific support for the centromeric drive theory. Cytogenet. Genome Res. 106: 347–350. https://doi.org/10.1159/000079311

Bilton, T. P., M. R. Schofield, M. A. Black, D. Chagné, P. L. Wilcox *et al.*, 2018 Accounting for errors in low coverage high-throughput sequencing data when constructing genetic maps using biparental outcrossed populations. Genetics 209: 65–76. https://doi.org/10.1534/genetics.117.300627

Blackmon, H., J. Justison, I. Mayrose, and E. E. Goldberg, 2019 Meiotic drive shapes rates of karyotype evolution in mammals. Evolution 73: 511–523. https://doi.org/10.1111/evo.13682

Bourque, G., and P. A. Pevzner, 2002 Genome-scale evolution: reconstructing gene orders in the ancestral species. Genome Res. 12: 26–36.

Bowers, J. E., E. Bachlava, R. L. Brunick, L. H. Rieseberg, S. J. Knapp *et al.*, 2012 Development of a 10,000 locus genetic map of the sunflower genome based on multiple crosses. G3 (Bethesda) 2: 721–729. https://doi.org/10.1534/g3.112.002659

Broman, K. W., H. Wu, S. Sen, and G. A. Churchill, 2003 R/qtl: QTL mapping in experimental crosses. Bioinformatics 19: 889–890. https://doi.org/10.1093/bioinformatics/btg112

Burke, J. M., Z. Lai, M. Salmaso, T. Nakazato, S. Tang *et al.*, 2004 Comparative mapping and rapid karyotypic evolution

in the genus *Helianthus*. Genetics 167: 449–457. https://doi.org/10.1534/genetics.167.1.449

Chandler, J. M., C. C. Jan, and B. H. Beard, 1986 Chromosomal differentiation among the annual *Helianthus* species. Syst. Bot. 11: 354–371. https://doi.org/10.2307/2419126

Chen, Z., B. Fu, M. Jiang, and B. Zhu, 2009 On recovering syntenic blocks from comparative maps. J. Comb. Optim. 18: 307–318. https://doi.org/10.1007/s10878-009-9233-x

Chmátal, L., S. I. Gabriel, G. P. Mitsainas, J. Martínez-Vargas, J. Ventura *et al*., 2014 Centromere strength provides the cell biological basis for meiotic drive and karyotype evolution in mice. Curr. Biol. 24: 2295–2300. https://doi.org/10.1016/j.cub.2014.08.017

Choi, V., C. Zheng, Q. Zhu, and D. Sankoff, 2007 Algorithms for the extraction of synteny blocks from comparative maps, pp. 277–288 in *International Workshop on Algorithms in Bioinformatics*. Springer, Berlin, Heidelberg. https://doi.org/10.1007/978-3-540-74126-8_26

Corbett-Detig, R. B., I. Said, M. Calzetta, M. Genetti, J. McBroome *et al*., 2019 Fine-mapping complex inversion breakpoints and investigating somatic pairing in the *Anopheles gambiae* species complex using proximity-ligation sequencing. Genetics 213: 1495–1511. https://doi.org/10.1534/genetics.119.302385

Danecek, P., A. Auton, G. Abecasis, C. A. Albers, E. Banks, *et al*., 2011 The variant call format and VCFtools. Bioinformatics 27: 2156–2158. https://doi.org/10.1093/bioinformatics/btr330

Darling, A. C. E., B. Mau, F. R. Blattner, and N. T. Perna, 2004 Mauve: multiple alignment of conserved genomic sequence with rearrangements. Genome Res. 14: 1394–1403. https://doi.org/10.1101/gr.2289704

DePristo, M. A., E. Banks, R. Poplin, K. V. Garimella, J. R. Maguire *et al*., 2011 A framework for variation discovery and genotyping using next-generation DNA sequencing data. Nat. Genet. 43: 491–498. https://doi.org/10.1038/ng.806

Doyle, J., and J. Doyle, 1987 A rapid DNA isolation procedure for small quantities of fresh leaf tissue. Phytochem. Bull. 19: 11–15.

Drillon, G., A. Carbone, and G. Fischer, 2014 SynChro: a fast and easy tool to reconstruct and visualize synteny blocks along eukaryotic chromosomes. PLoS One 9: e92621. https://doi.org/10.1371/journal.pone.0092621

Dvorak, J., L. Wang, T. Zhu, C. M. Jorgensen, K. R. Deal *et al*., 2018 Structural variation and rates of genome evolution in the grass family seen through comparison of sequences of genomes greatly differing in size. Plant J. 95: 487–503. https://doi.org/10.1111/tpj.13964

Ferguson-Smith, M. A., and V. Trifonov, 2007 Mammalian karyotype evolution. Nat. Rev. Genet. 8: 950–962. https://doi.org/10.1038/nrg2199

Ferriera, J. V., 1980 Introgressive hybridization between *Helanthus annuus* L. and *Helianthus petiolaris* Nutt. Mendeliana 4: 81–93.

Fishman, L., A. Stathos, P. M. Beardsley, C. F. Williams, and J. P. Hill, 2013 Chromosomal rearrangements and the genetics of reproductive barriers in *Mimulus* (monkey flowers). Evolution 67: 2547–2560. https://doi.org/10.1111/evo.12154

Flagel, L. E., B. K. Blackman, L. Fishman, P. J. Monnahan, A. Sweigart *et al*., 2019 GOOGA: a platform to synthesize mapping experiments and identify genomic structural diversity. PLoS Comput. Biol. 15: e1006949. https://doi.org/10.1371/journal.pcbi.1006949

Goel, M., H. Sun, W. B. Jiao, and K. Schneeberger, 2019 SyRI: finding genomic rearrangements and local sequence differences from whole-genome assemblies. Genome Biol. 20: 277. https://doi.org/10.1186/s13059-019-1911-0

Hackett, C. A., and L. B. Broadfoot, 2003 Effects of genotyping errors, missing values and segregation distortion in molecular marker data on the construction of linkage maps. Heredity 90: 33–38. https://doi.org/10.1038/sj.hdy.6800173

Hardison, R. C., K. M. Roskin, S. Yang, M. Diekhans, W. J. Kent *et al*., 2003 Covariation in frequencies of substitution, deletion, transposition, and recombination during eutherian evolution. Genome Res. 13: 13–26. https://doi.org/10.1101/gr.844103

Heesacker, A. F., E. Bachlava, R. L. Brunick, J. M. Burke, L. H. Rieseberg *et al*., 2009 Karyotypic evolution of the common and silverleaf sunflower genomes. Plant Genome 2: 233–246. https://doi.org/10.3835/plantgenome2009.05.0015

Heiser, C. B., Jr., 1947 Hybridization between the sunflower species *Helianthus annuus* and *H. petiolaris*. Evolution 1: 249–262. https://doi.org/10.1111/j.1558-5646.1947.tb02722.x

Heiser, C. B., Jr., 1948 Taxonomic and cytological notes on the annual species of *Helianthus*. Bull. Torrey Bot. Club 75: 512–515. https://doi.org/10.2307/2481785

Heiser, C. B., Jr., 1951 Hybridization in the annual sunflowers: *Helianthus annuus* x *H. argophyllus*. Am. Nat. 85: 65–72. https://doi.org/10.1086/281651

Heiser, C. B., Jr., 1961 Morphological and cytological variation in *Helianthus petiolaris* with notes on related species. Evolution 15: 247–258. https://doi.org/10.1111/j.1558-5646.1961.tb03147.x

Hoffmann, A. A., and L. H. Rieseberg, 2008 Revisiting the impact of inversions in evolution: from population genetic markers to drivers of adaptive shifts and speciation? Annu. Rev. Ecol. Evol. Syst. 39: 21–42. https://doi.org/10.1146/annurev.ecolsys.39.110707.173532

Huang, S., R. Li, Z. Zhang, L. Li, X. Gu *et al*., 2009 The genome of the cucumber, *Cucumis sativus* L. Nat. Genet. 41: 1275–1281. https://doi.org/10.1038/ng.475

Huang K., R. L. Andrew, G. L. Owens, K. L. Ostevik, and L. H. Rieseberg, 2019 Multiple chromosomal inversions contribute to adaptive divergence of a dune sunflower ecotype. bioRxiv. Available at: https://www.biorxiv.org/content/10.1101/829622v1.full. Accessed: December 30, 2019. doi: 10.1101/829622https://doi.org/10.1101/829622

Huchra, J. P., and M. J. Geller, 1982 Groups of galaxies. I. Nearby groups. Astrophys. J. 257: 423–437. https://doi.org/10.1086/160000

International Brachypodium Initiative, *et al*., 2010 Genome sequencing and analysis of the model grass Brachypodium distachyon. Nature 463: 763–768. https://doi.org/10.1038/nature08747

Joshi, N. A., 2011 Sabre: A barcode demultiplexing and trimming tool for FastQ files. https://github.com/najoshi/sabre. Accessed: January 27, 2017.

Kaszás, E., and J. A. Birchler, 1998 Meiotic transmission rates correlate with physical features of rearranged centromeres in maize. Genetics 150: 1683–1692.

Kawabe, A., B. Hansson, J. Hagenblad, A. Forrest, and D. Charlesworth, 2006 Centromere locations and associated chromosome rearrangements in *Arabidopsis lyrata* and *A. thaliana*. Genetics 173: 1613–1619. https://doi.org/10.1534/genetics.106.057182

Kawakami, T., P. Dhakal, A. N. Katterhenry, C. A. Heatherington, and M. C. Ungerer, 2011 Transposable element proliferation and genome expansion are rare in contemporary sunflower hybrid populations despite widespread transcriptional activity of LTR retrotransposons. Genome Biol. Evol. 3: 156–167. https://doi.org/10.1093/gbe/evr005

King, M., 1987 Chromosomal rearrangements, speciation and the theoretical approach. Heredity 59: 1–6. https://doi.org/10.1038/hdy.1987.90

King, M., 1993 *Species Evolution*, Cambridge University Press, Cambridge.

Kirkpatrick, M., and N. Barton, 2006 Chromosome inversions, local adaptation and speciation. Genetics 173: 419–434 [corrigenda: Genetics 208: 433 (2018)]. https://doi.org/10.1534/genetics.105.047985

Lai, Z., T. Nakazato, M. Salmaso, J. M. Burke, S. Tang *et al.*, 2005 Extensive chromosomal repatterning and the evolution of sterility barriers in hybrid sunflower species. Genetics 171: 291–303. https://doi.org/10.1534/genetics.105.042242

Larkin, D. M., G. Pape, R. Donthu, L. Auvil, M. Welge *et al.*, 2009 Breakpoint regions and homologous synteny blocks in chromosomes have different evolutionary histories. Genome Res. 19: 770–777. https://doi.org/10.1101/gr.086546.108

Latta, R. G., W. A. Bekele, C. P. Wight, and N. A. Tinker, 2019 Comparative linkage mapping of diploid, tetraploid, and hexaploid Avena species suggests extensive chromosome rearrangement in ancestral diploids. Sci. Rep. 9: 12298. https://doi.org/10.1038/s41598-019-48639-7

Li H., 2013 Aligning sequence reads, clone sequences and assembly contigs with BWA-MEM. arXiv. Available: https://arxiv.org/abs/1303.3997. (accessed January 27, 2017) doi: 1303.3997v2 https://doi.org/doi: 1303.3997v2

Li, H., and R. Durbin, 2010 Fast and accurate long-read alignment with Burrows-Wheeler transform. Bioinformatics 26: 589–595. https://doi.org/10.1093/bioinformatics/btp698

Li, S.-F., T. Su, G.-Q. Cheng, B.-X. Wang, X. Li *et al.*, 2017 Chromosome evolution in connection with repetitive sequences and epigenetics in plants. Genes (Basel) 8: 290. https://doi.org/10.3390/genes8100290

Lin, C.-Y., A. Shukla, J. P. Grady, J. L. Fink, E. Dray *et al.*, 2018 Translocation breakpoints preferentially occur in euchromatin and acrocentric chromosomes. Cancers (Basel) 10: 13. https://doi.org/10.3390/cancers10010013

Mandel, J. R., S. Nambeesan, J. E. Bowers, L. F. Marek, D. Ebert *et al.*, 2013 Association mapping and the genomic consequences of selection in sunflower. PLoS Genet. 9: e1003378. https://doi.org/10.1371/journal.pgen.1003378

Marone, D., G. Laidò, A. Gadaleta, P. Colasuonno, D. B. M. Ficco *et al.*, 2012 A high-density consensus map of A and B wheat genomes. Theor. Appl. Genet. 125: 1619–1638. https://doi.org/10.1007/s00122-012-1939-y

Martinez, P. A., U. P. Jacobina, R. V. Fernandes, C. Brito, C. Penone *et al.*, 2016 A comparative study on karyotypic diversification rate in mammals. Heredity 118: 366–373. https://doi.org/10.1038/hdy.2016.110

Mason, C. M., 2018 How old are sunflowers? A molecular clock analysis of key divergences in the origin and diversification of *Helianthus* (Asteraceae). Int. J. Plant Sci. 179: 182–191. https://doi.org/10.1086/696366

Mason, A. S., M. N. Nelson, J. Takahira, W. A. Cowling, G. M. Alves *et al.*, 2014 The fate of chromosomes and alleles in an allohexaploid *Brassica* population. Genetics 197: 273–283. https://doi.org/10.1534/genetics.113.159574

Matvienko, M., A. Kozik, L. Froenicke, D. Lavelle, B. Martineau *et al.*, 2013 Consequences of normalizing transcriptomic and genomic libraries of plant genomes using a duplex-specific nuclease and tetramethylammonium chloride. PLoS One 8: e55913. https://doi.org/10.1371/journal.pone.0055913

McKenna, A., M. Hanna, E. Banks, A. Sivachenko, K. Cibulskis *et al.*, 2010 The Genome Analysis Toolkit: a MapReduce framework for analyzing next-generation DNA sequencing data. Genome Res. 20: 1297–1303. https://doi.org/10.1101/gr.107524.110

Molina, W. F., P. A. Martinez, L. A. C. Bertollo, and C. J. Bidau, 2014 Evidence for meiotic drive as an explanation for karyotype changes in fishes. Mar. Genomics 15: 29–34. https://doi.org/10.1016/j.margen.2014.05.001

Molnár, I., M. Cifuentes, A. Schneider, E. Benavente, and M. Molnár-Láng, 2010 Association between simple sequence repeat-rich chromosome regions and intergenomic translocation breakpoints in natural populations of allopolyploid wild wheats. Ann. Bot. (Lond.) 107: 65–76. https://doi.org/10.1093/aob/mcq215

Murphy, W. J., D. M. Larkin, A. Everts-van der Wind, G. Bourque, G. Tesler *et al.*, 2005 Dynamics of mammalian chromosome evolution inferred from multispecies comparative maps. Science 309: 613–617. https://doi.org/10.1126/science.1111387

Nagaki, K., K. Tanaka, N. Yamaji, H. Kobayashi, and M. Murata, 2015 Sunflower centromeres consist of a centromere-specific LINE and a chromosome-specific tandem repeat. Front. Plant Sci. 6: 912. https://doi.org/10.3389/fpls.2015.00912

Navarro, A., and N. H. Barton, 2003 Chromosomal speciation and molecular divergence–accelerated evolution in rearranged chromosomes. Science 300: 321–324. https://doi.org/10.1126/science.1080600

Nguepjop, J. R., H.-A. Tossim, J. M. Bell, J.-F. Rami, S. Sharma *et al.*, 2016 Evidence of genomic exchanges between homeologous chromosomes in a cross of peanut with newly synthetized allotetraploid hybrids. Front. Plant Sci. 7: 1635. https://doi.org/10.3389/fpls.2016.01635

Nicolas, S. D., G. L. Mignon, F. Eber, O. Coriton, H. Monod *et al.*, 2007 Homeologous recombination plays a major role in chromosome rearrangements that occur during meiosis of *Brassica napus* haploids. Genetics 175: 487–503. https://doi.org/10.1534/genetics.106.062968

Noor, M. A., K. L. Grams, L. A. Bertucci, and J. Reiland, 2001 Chromosomal inversions and the reproductive isolation of species. Proc. Natl. Acad. Sci. USA 98: 12084–12088. https://doi.org/10.1073/pnas.221274498

Okita, A. K., F. Zafar, J. Su, D. Weerasekara, T. Kajitani *et al.*, 2019 Heterochromatin suppresses gross chromosomal rearrangements at centromeres by repressing Tfs1/TFIIS-dependent transcription. Commun. Biol. 2: 17. https://doi.org/10.1038/s42003-018-0251-z

Oliveira da Silva, W., J. C. Pieczarka, M. J. Rodrigues da Costa, M. A. Ferguson-Smith, P. C. M. O'Brien *et al.*, 2019 Chromosomal phylogeny and comparative chromosome painting among Neacomys species (Rodentia, Sigmodontinae) from eastern Amazonia. BMC Evol. Biol. 19: 184. https://doi.org/10.1186/s12862-019-1515-z

Ostevik K. L., 2016 The ecology and genetics of adaptation and speciation in dune sunflowers. Ph.D. Thesis, University of Toronto, Toronto.

Ouellette, L. A., R. W. Reid, S. G. Blanchard, and C. R. Brouwer, 2017 LinkageMapView - rendering high resolution linkage and QTL maps. Bioinformatics 34: 306–307. https://doi.org/10.1093/bioinformatics/btx576

Palestis, B. G., A. Burt, R. N. Jones, and R. Trivers, 2004 B chromosomes are more frequent in mammals with acrocentric karyotypes: support for the theory of centromeric drive. Proc. Biol. Sci. 271: S22–S24. https://doi.org/10.1098/rsbl.2003.0084

Pevzner, P., and G. Tesler, 2003 Genome rearrangements in mammalian evolution: lessons from human and mouse genomes. Genome Res. 13: 37–45. https://doi.org/10.1101/gr.757503

Poland, J. A., P. J. Brown, M. E. Sorrells, and J. L. Jannink, 2012 Development of high-density genetic maps for barley and wheat using a novel two-enzyme genotyping-by-sequencing approach. PLoS One 7: e32253. https://doi.org/10.1371/journal.pone.0032253

Quillet, M. C., N. Madjidian, Y. Griveau, H. Serieys, M. Tersac *et al.*, 1995 Mapping genetic factors controlling pollen viability in an interspecific cross in *Helianthus* sect. *Helianthus*. Theor. Appl. Genet. 91: 1195–1202. https://doi.org/10.1007/BF00220929

Raduski, A. R., L. Rieseberg, and J. Strasburg, 2010 Effective population size, gene flow, and species status in a narrow endemic sunflower, *Helianthus neglectus*, compared to its widespread sister species, *H. petiolaris*. IJMS 11: 492–506. https://doi.org/10.3390/ijms11020492

Raskina, O., J. C. Barber, E. Nevo, and A. Belyayev, 2008 Repetitive DNA and chromosomal rearrangements: speciation-related events in plant genomes. Cytogenet. Genome Res. 120: 351–357. https://doi.org/10.1159/000121084

Rieseberg, L. H., 1991 Homoploid reticulate evolution in *Helianthus* (Asteraceae): evidence from ribosomal genes. Am. J. Bot. 78: 1218–1237. https://doi.org/10.1002/j.1537-2197.1991.tb11415.x

Rieseberg, L. H., 2001 Chromosomal rearrangements and speciation. Trends Ecol. Evol. 16: 351–358. https://doi.org/10.1016/S0169-5347(01)02187-5

Rieseberg, L. H., C. R. Linder, and G. J. Seiler, 1995 Chromosomal and genic barriers to introgression in *Helianthus*. Genetics 141: 1163–1171.

Rogers, C. E., T. E. Thompson, and G. J. Seiler, 1982 *Sunflowers Species of the United States*. National Sunflower Association, Mandan, ND.

Rohland, N., and D. Reich, 2012 Cost-effective, high-throughput DNA sequencing libraries for multiplexed target capture. Genome Res. 22: 939–946. https://doi.org/10.1101/gr.128124.111

Rueppell, O., R. Kuster, K. Miller, B. Fouks, S. Rubio Correa *et al*., 2016 A new metazoan recombination rate record and consistently high recombination rates in the honey bee genus *Apis* accompanied by frequent inversions but not translocations. Genome Biol. Evol. 8: 3653–3660.

Sambatti, J. B. M., J. L. Strasburg, D. Ortiz-Barrientos, E. J. Baack, and L. H. Rieseberg, 2012 Reconciling extremely strong barriers with high levels of gene exchange in annual sunflowers. Evolution 66: 1459–1473. https://doi.org/10.1111/j.1558-5646.2011.01537.x

Schlautman, B., L. Diaz-Garcia, G. Covarrubias-Pazaran, N. Schlautman, N. Vorsa *et al*., 2017 Comparative genetic mapping reveals synteny and collinearity between the American cranberry and diploid blueberry genomes. Mol. Breed. 38: 9.

Schranz, M. E., T. Mitchell-Olds, and M. A. Lysak, 2006 The ABC's of comparative genomics in the Brassicaceae: building blocks of crucifer genomes. Trends Plant Sci. 11: 535–542. https://doi.org/10.1016/j.tplants.2006.09.002

Searle, J. B., 1993 Chromosomal hybrid zones in eutherian mammals, pp. 309–353 in *Hybrid Zones and the Evolutionary Process*, edited by R. G. Harrison, Oxford University Press on Demand, Oxford.

Shagina, I., E. Bogdanova, I. Mamedov, Y. Lebedev, S. Lukyanov *et al*., 2010 Normalization of genomic DNA using duplex-specific nuclease. Biotechniques 48: 455–459. https://doi.org/10.2144/000113422

Sinha, A. U., and J. Meller, 2007 Cinteny: flexible analysis and visualization of synteny and genome rearrangements in multiple organisms. BMC Bioinformatics 8: 82. https://doi.org/10.1186/1471-2105-8-82

Soderlund, C., Bomhoff, M., and W. M. Nelson, 2011 SyMAP v3.4: a turnkey synteny system with application to plant genomes. Nucleic Acids Res. 39: e68. https://doi.org/10.1093/nar/gkr123

Stathos, A., and L. Fishman, 2014 Chromosomal rearrangements directly cause underdominant F1 pollen sterility in *Mimulus lewisii-Mimulus cardinalis* hybrids. Evolution 68: 3109–3119. https://doi.org/10.1111/evo.12503

Staton, S. E., B. H. Bakken, B. K. Blackman, M. A. Chapman, N. C. Kane *et al*., 2012 The sunflower (*Helianthus annuus* L.) genome reflects a recent history of biased accumulation of transposable elements. Plant J. 72: 142–153. https://doi.org/10.1111/j.1365-313X.2012.05072.x

Stephens, J. D., W. L. Rogers, C. M. Mason, L. A. Donovan, and R. L. Malmberg, 2015 Species tree estimation of diploid *Helianthus* (Asteraceae) using target enrichment. Am. J. Bot. 102: 910–920. https://doi.org/10.3732/ajb.1500031

Strasburg, J., and L. Rieseberg, 2008 Molecular demographic history of the annual sunflowers *Helianthus annuus* and *H. petiolaris*—large effective population sizes and rates of long-term gene flow. Evolution 62: 1936–1950. https://doi.org/10.1111/j.1558-5646.2008.00415.x

Sun, S., V. Yadav, R. B. Billmyre, C. A. Cuomo, M. Nowrousian *et al*., 2017 Fungal genome and mating system transitions facilitated by chromosomal translocations involving intercentromeric recombination. PLoS Biol. 15: e2002527. https://doi.org/10.1371/journal.pbio.2002527

Tang, S., J. K. Yu, M. B. Slabaugh, D. K. Shintani, and S. J. Knapp, 2002 Simple sequence repeat map of the sunflower genome. TAG Theoretical and Applied Genetics 105: 1124–1136. https://doi.org/10.1007/s00122-002-0989-y

Taylor, J., and D. Butler, 2017 R Package ASMap: efficient genetic linkage map construction and diagnosis. J. Stat. Softw. 79: 1–29. https://doi.org/10.18637/jss.v079.i06

Tennessen, J. A., R. Govindarajulu, T. L. Ashman, and A. Liston, 2014 Evolutionary origins and dynamics of octoploid strawberry subgenomes revealed by dense targeted capture linkage maps. Genome Biol. Evol. 6: 3295–3313. https://doi.org/10.1093/gbe/evu261

Todesco M., G. L. Owens, N. Bercovich, J. S. Légaré, S. Soudi *et al.* 2019 Massive haplotypes underlie ecotypic differentiation in sunflowers. bioRxiv. Available at: https://www.biorxiv.org/content/10.1101/790279v1. Accessed December 30, 2019. doi: 10.1101/79027https://doi.org/10.1101/79027

Trickett, A. J., and R. K. Butlin, 1994 Recombination suppressors and the evolution of new species. Heredity 73: 339–345. https://doi.org/10.1038/hdy.1994.180

Van der Auwera G. A., M. O. Carneiro, C. Hartl, R. Poplin, G. Del Angel *et al*., 2013 From FastQ data to high-confidence variant calls: The Genome Analysis Toolkit best practices pipeline. Curr. Protoc. Bioinformatics 43: 11.10.1–11.10.33.

Vitte, C., M. A. Fustier, K. Alix, and M. I. Tenaillon, 2014 The bright side of transposons in crop evolution. Brief. Funct. Genomics 13: 276–295. https://doi.org/10.1093/bfgp/elu002

Weiss-Schneeweiss, H., and G. M. Schneeweiss, 2012 Karyotype diversity and evolutionary trends in angiosperms, pp. 209–230 in *Plant Genome Diversity Volume 2: Physical Structure, Behaviour and Evolution of Plant Genomes*. Edited by I. J. Leitch, J. Greilhuber, J. Doležel, and J. F. Wendel. Springer-Verlag, Heidelberg.

Whelan, E. D., 1979 Interspecific hybrids between *Helianthus petiolaris* Nutt. and *H. annuus* L.: effect of backcrossing on meiosis. Euphytica 28: 297–308. https://doi.org/10.1007/BF00056586

White, M. J. D., 1973 *Animal Cytology and Evolution*. Cambridge University Press, Cambridge.

White, M. J. D., 1978 *Modes of Speciation*. W. H. Freeman & Co., San Francisco.

Wu, F., and S. D. Tanksley, 2010 Chromosomal evolution in the plant family Solanaceae. BMC Genomics 11: 182. https://doi.org/10.1186/1471-2164-11-182

Yeaman, S., 2013 Genomic rearrangements and the evolution of clusters of locally adaptive loci. Proc. Natl. Acad. Sci. USA 110: E1743–E1751. https://doi.org/10.1073/pnas.1219381110

Yeaman, S., and M. Whitlock, 2011 The genetic architecture of adaptation under migration-selection balance. Evolution 65: 1897–1911. https://doi.org/10.1111/j.1558-5646.2011.01269.x

Yogeeswaran, K., A. Frary, T. L. York, A. Amenta, A. H. Lesser *et al*., 2005 Comparative genome analyses of *Arabidopsis* spp.: inferring chromosomal rearrangement events in the evolutionary history of *A. thaliana*. Genome Res. 15: 505–515. https://doi.org/10.1101/gr.3436305

Zanders, S. E., M. T. Eickbush, J. S. Yu, J. W. Kang, K. R. Fowler *et al*., 2014 Genome rearrangements and pervasive meiotic drive cause hybrid infertility in fission yeast. Elife 3: e02630. https://doi.org/10.7554/eLife.02630

Zhulidov, P. A., E. A. Bogdanova, A. S. Shcheglov, L. L. Vagner, G. L. Khaspekov *et al*., 2004 Simple cDNA normalization using kamchatka crab duplex-specific nuclease. Nucleic Acids Res. 32: e37. https://doi.org/10.1093/nar/gnh031

*Communicating editor: L. Moyle*